Electronic Supplementary Information (ESI) for

Ternary ZIF-8-derived dual-metal CoCu nanoparticles in porous carbon polyhedrons as efficient catalysts for methanol oxidation

Chaoyun Tang[a,b,c] and *Tewodros Asefa*[*b,c]

[a] *Hoffmann Institute of Advanced Materials, Shenzhen Polytechnic, 7098 Liuxian Boulevard, Nanshan District, Shenzhen 518060, China*

[b] *Department of Chemistry and Chemical Biology, Rutgers, The State University of New Jersey, 610 Taylor Road, Piscataway, New Jersey 08854, USA*

E-mail: tasefa@chem.rutgers.edu

[c] *Department of Chemical & Biochemical Engineering, Rutgers, The State University of New Jersey, 98 Brett Road, Piscataway, New Jersey 08854, USA*

Experimental Procedures

Chemical and Reagents

Zinc(II) nitrate hexahydrate ($Zn(NO_3)_2 \cdot 6H_2O$), cobalt(II) nitrate hexahydrate ($Co(NO_3)_2 \cdot 6H_2O$), copper(II) nitrate hemi(pentahydrate) ($Cu(NO_3)_2 \cdot 2.5H_2O$), and 2-methylimidazole (2-MeMi, $C_4H_6N_2$) were purchased from Sigma-Aldrich. They were all used as received and without further purification.

Synthesis of Ternary ZIFs

Ternary ZIFs microparticles were synthesized by following a procedure reported for ZIF-8,[1,2] with a slight modification. Most notably, the ternary ZIFs were synthesized in one-step. In a typical synthesis, solutions of three different divalent cationic metals (Zn^{2+}, Co^{2+}, and Cu^{2+}) in different ratios, namely Zn:Co:Cu = 6:4:0; 6:3:1; 6:2:2; 6:1:3; and 6:0:4 (the total amount of which is 4 mmol), in 40 mL deionized water were prepared. Each solution was rapidly added into another one prepared by mixing 2-MeMi (150 mmol) and 150 mL deionized water. The solution was vigorously stirred for 24 h. The resulting solid products were collected by centrifuging the solution at 7500 rpm for 10 min. The products were washed with deionized water and then ethanol, three times in each case. They were dried at 60 °C overnight, giving different ZIFs with different types of metals and relative amounts of Zn, Co and Cu.

Synthesis of 3D Nanoporous Carbon Polyhedrons Containing CoCu Nanoparticles

Each ZIF material prepared above was placed in an alumina boat in a tube furnace and pyrolyzed in a nitrogen (N_2) atmosphere from room temperature to 900 °C at a rate of 5 °C per minute and kept at 900 °C for 3 h. During the pyrolysis process, Zn, which has a lower boiling point, evaporated above 800 °C while Co and Cu remained with the carbon material. It is worth noting here that the pyrolysis was done at 900 °C for 3 h to ensure the complete removal of Zn element while keeping the well-defined morphology and structures of the MOF-derived carbon skeleton intact. Most ZIF-derived carbon materials reported previously were also synthesized through pyrolysis at 900 °C for 3 h.[3,4] The pyrolysis finally gave different 3D nanoporous polyhedral-shaped carbon microparticles containing Co and Cu nanoparticles in different ratios. The corresponding control materials possessing either only Co or only Cu, were also obtained with the same procedure. The materials were all named as carbonized ZIFs (or CZIFs). To differentiate the materials from one another, subscripts along with the two metals were included with their names, denoted as "CZIF(Co_xCu_y)", where x:y represent the ratio of the two metals used to make their parent ZIFs.

Characterizations

Powder X-ray diffraction (XRD) patterns of the materials were recorded using a Bruker X-ray diffractometer (D8 advance) operating with a Cu Kα X-ray source (λ = 0.154 nm) to analyze their crystal structures. A field-emission scanning electron microscope (FESEM) (Zeiss Supra 55) equipped with energy dispersive X-ray spectroscopy (EDS) was used to determine the morphology, structures and elemental composition of the materials. The morphology and microstructure of the materials were further investigated with a JEM-6700F transmission electron microscope (TEM) (JEOL) and a JEM-6700F high-resolution transmission electron microscope (HRTEM) (JEOL). Using the same microscope, selected-area electron diffraction (SAED) patterns were acquired to study the crystal structure of samples. The porosity of the materials was analyzed with N_2 adsorption/desorption at 77 K using a Quantachrome instrument (Autosorb-IQ2-MP). The surface compositions of the materials were analyzed with a model ESCALAB 250 Xi X-ray photoelectron spectrometer (XPS) (Thermo Scientific).

Electrochemical Measurements and Electrocatalysis

All the electrochemical and electrocatalytic measurements were conducted with an electrochemical setup comprising a VersaSTAT 3 Potentiostat Galvanostat (Princeton Applied Research) and a VersaStudio software at ambient environment. In the electrochemical cell, a glassy carbon electrode (GCE) with diameter of 3 mm containing catalyst was used as a working electrode, a carbon rod was used as a counter electrode, and a saturated calomel electrode (SCE) was used as a reference electrode. To prepare the working electrode, first 2 mg catalyst was dispersed in a solution of deionized water and ethanol (with a volume ratio of 4:1, 1 mL,) and Nafion solution (80 μL) with ultrasonication for 30 min. Then, 5 μL of the slurry was drop-casted onto a GCE and dried in air. The amount of each catalyst on the working electrode was kept the same (0.2 mg cm^{-2}) in order to easily compare their properties.

An aqueous 1 M KOH solution and an aqueous 1 M KOH + 1 M MeOH solution were used as electrolytes for cyclic voltammetry (CV) and MOR experiments. The potential was scanned in the range of 0.2 to 1 V vs. SCE at a scan rate of 50 mV s^{-1}. Before each measurement, the electrolyte was purged with N_2 gas to remove dissolved oxygen (O_2) in it. The current densities due to MOR were measured with respect to the geometric area of the GCE. The data obtained from the measurements were all corrected for iR losses and background currents. Electrochemical impedance spectroscopy (EIS) was performed with a voltage amplitude of 5 mV at frequencies in the range of 100 kHz to 100 Hz. To determine the electrochemical capacitance of each material, experiments were performed by sweeping the

potential three times in the non-Faradaic region of 0.2 to 0.3 V vs. RHE. These experiments were done at seven different scan rates, namely, 20, 40, 60, 80, 100, 120 and 140 mV s^{-1}.

Additional Results and Discussions

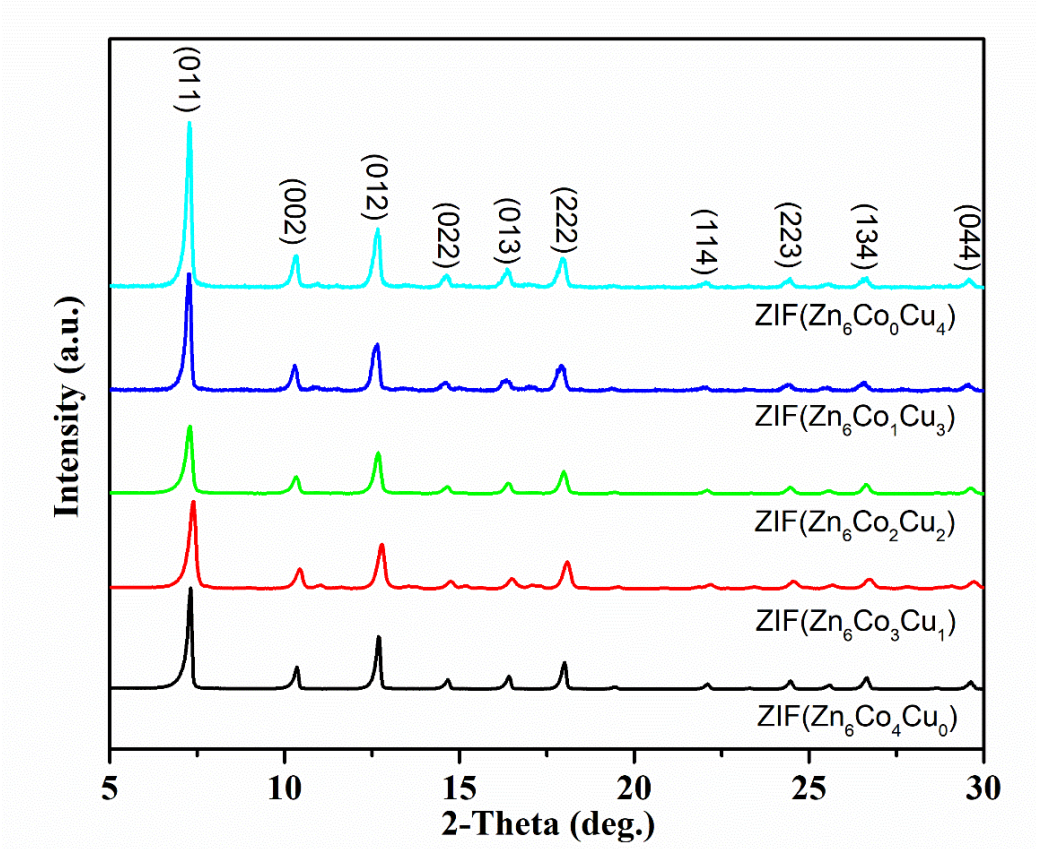

Figure S1. Powder XRD patterns of as-synthesized ternary metal ZIF materials prepared with different mole ratios of Zn, Co and Cu.

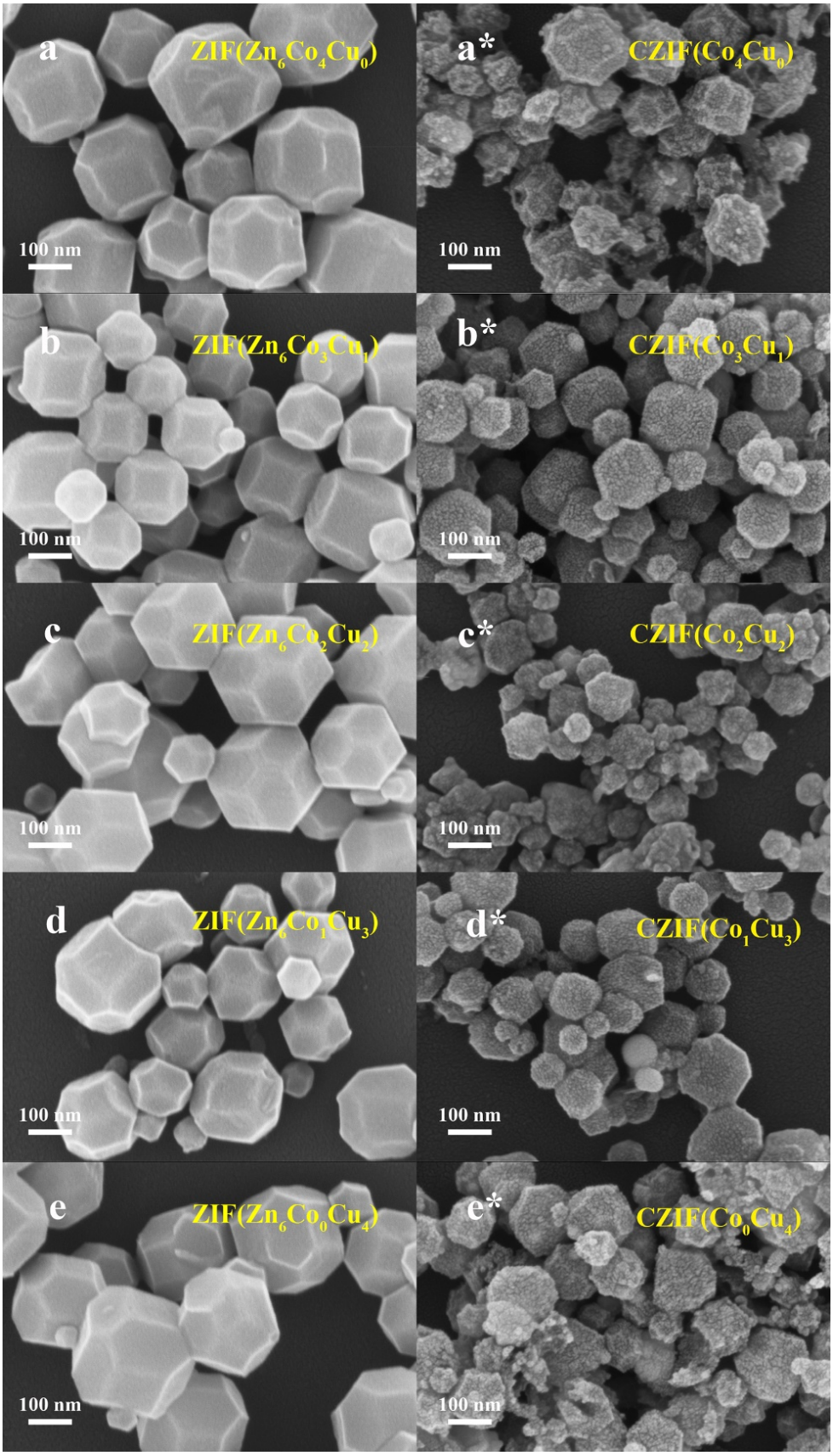

Figure S2. (Left panels) FESEM images of a series ZIF materials prepared from different mole ratios of Zn, Co and Cu. (Right panels) FESEM images of the corresponding CZIF materials containing different amounts of Co and Cu.

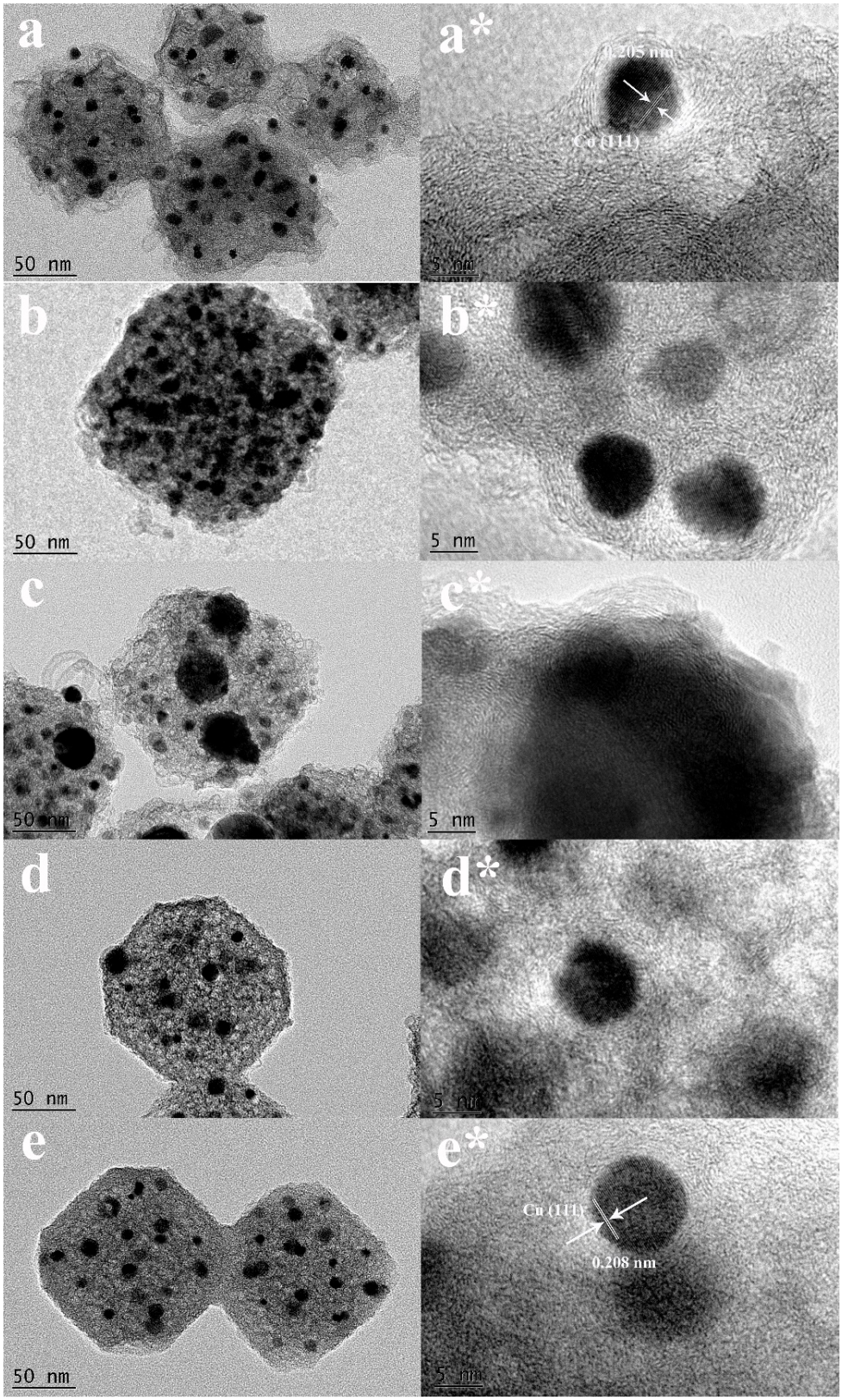

Figure S3. High-resolution transmission electron microscope (HRTEM) images in different magnification of different CZIF materials synthesized with different amounts of Co and Cu, namely: (a,a*) CZIF(Co_4Cu_0); (b,b*) CZIF(Co_3Cu_1); (c,c*) CZIF(Co_2Cu_2); (d,d*) CZIF(Co_1Cu_3); and (e,e*) CZIF(Co_0Cu_4).

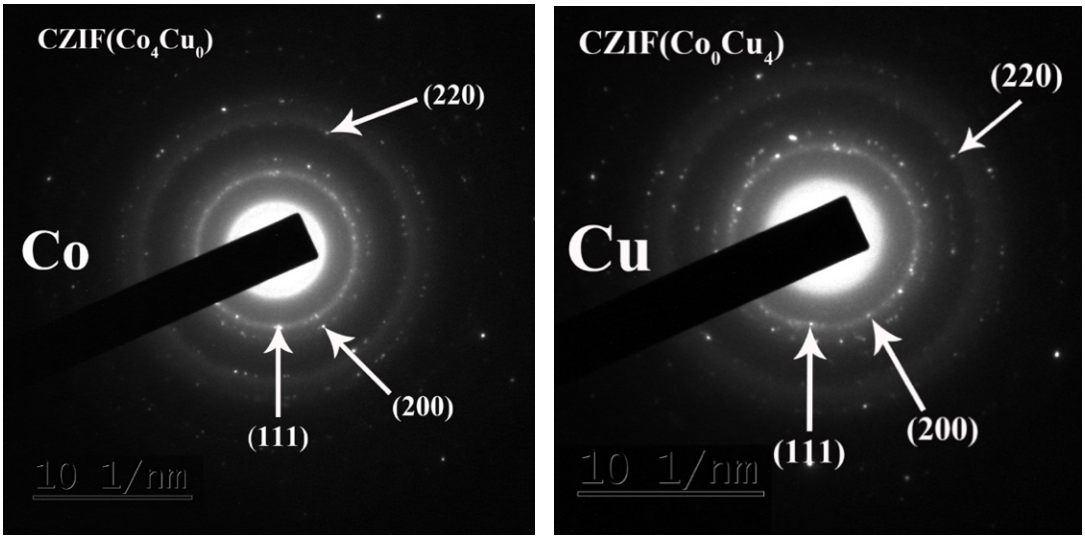

Figure S4. Selected area electron diffraction (SAED) patterns of CZIF(Co_4Cu_0) (left panel) and CZIF(Co_0Cu_4) (right panel). These two materials contain only Co or only Cu nanoparticles, respectively.

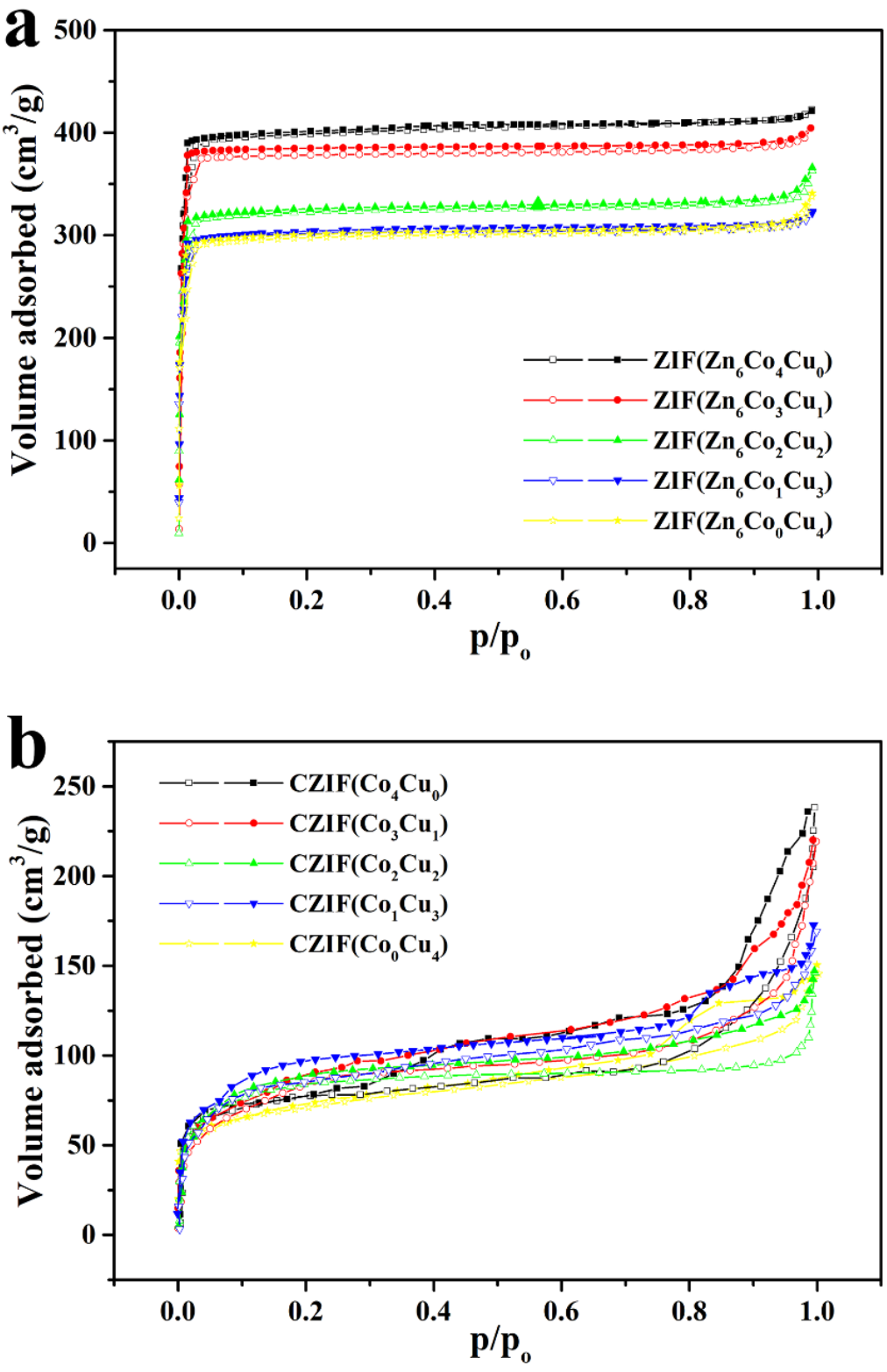

Figure S5. Nitrogen (N_2) adsorption/desorption isotherms of (a) a series ZIF materials containing different amounts of Zn, Co and Cu and (b) the corresponding CZIF materials containing different amounts of Co and Cu.

Table S1. Porosity data of various ZIF and CZIF materials synthesized and studied herein.

Samples	BET Surface Area (S_{BET}) ($m^2\ g^{-1}$) [a]	Total Pore Volume (V_{total}) ($cm^3\ g^{-1}$) [b]	Average Pore Diameter (D_{pore}) (nm) [c]
ZIF($Zn_6Co_4Cu_0$)	1831	0.66	2.13
ZIF($Zn_6Co_3Cu_1$)	1724	0.62	2.02
ZIF($Zn_6Co_2Cu_2$)	1320	0.53	1.92
ZIF($Zn_6Co_1Cu_3$)	1250	0.48	1.83
ZIF($Zn_6Co_0Cu_4$)	1216	0.47	1.80
CZIF(Co_4Cu_0)	314	0.37	7.97
CZIF(Co_3Cu_1)	298	0.35	7.53
CZIF(Co_2Cu_2)	268	0.31	6.52
CZIF(Co_1Cu_3)	275	0.31	6.18
CZIF(Co_0Cu_4)	288	0.32	6.06

[a] Specific surface area calculated by the Brunauer-Emmett-Teller (BET) method. [b] Total pore volume at P/P_o = 0.95. [c] Data calculated by the non-local density functional theory (NLDFT) method.

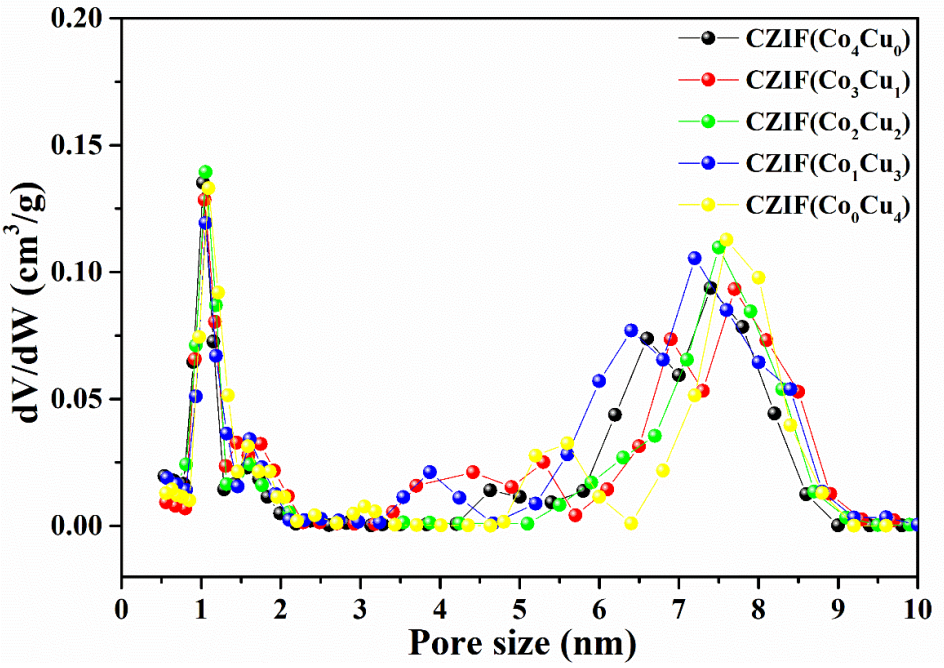

Figure S6. Pore size distributions of different CZIF materials containing different amounts of Co and Cu.

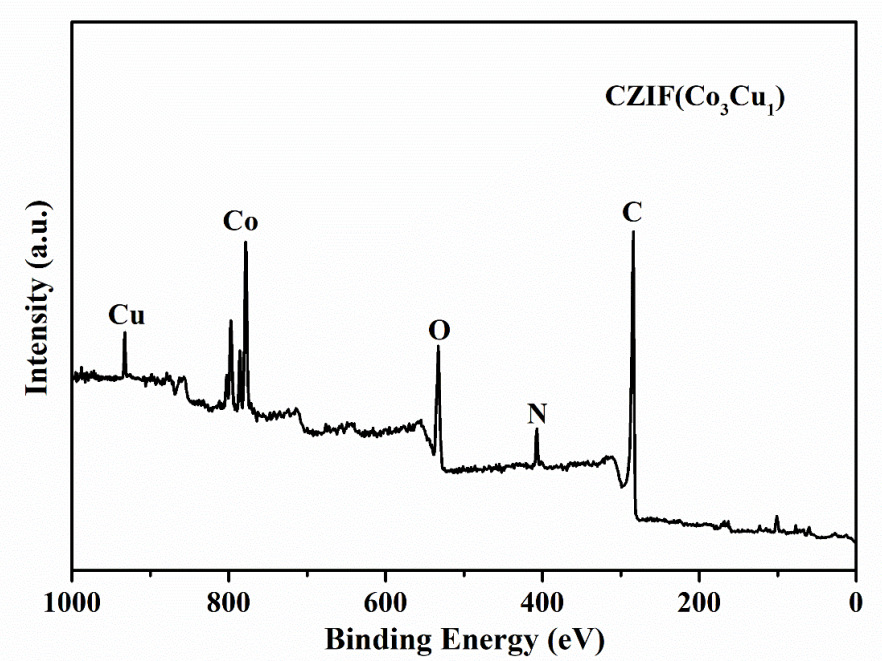

Figure S7. A survey XPS spectrum of an as-synthesized CZIF(Co_3Cu_1) material.

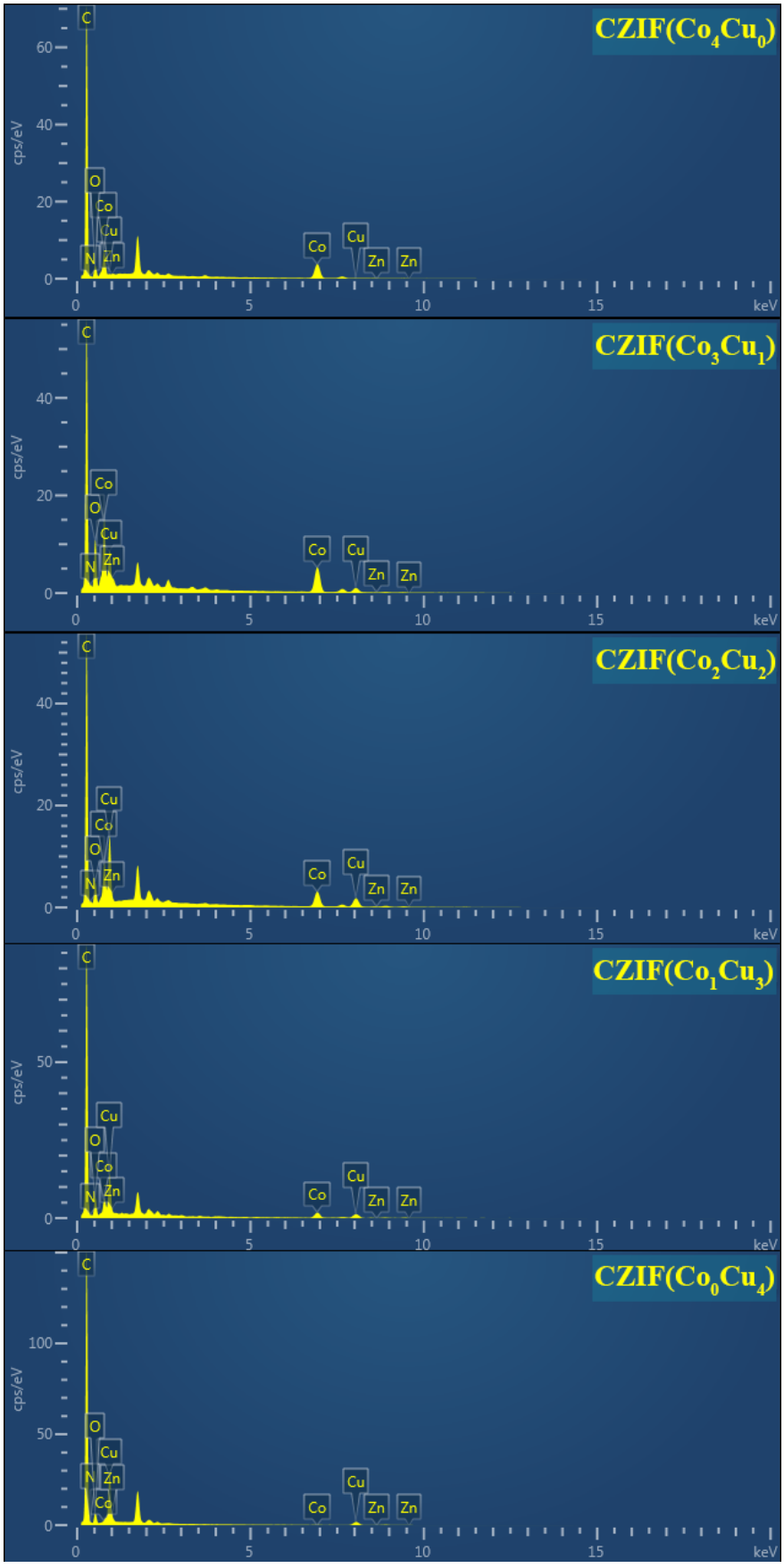

Figure S8. Energy dispersive X-ray spectra (EDS) of different CZIF materials prepared with different amounts of Co and Cu.

Table S2. The relative amounts of different elements in different CZIF materials. The analysis is based on the EDS spectra of the materials.

Samples	Elements (wt. %)						
	C	N	O	Co	Cu	Zn	Total amount
CZIF(Co_4Cu_0)	71.01	1.13	5.46	21.92	0	0.49	~100
CZIF(Co_3Cu_1)	72.33	1.11	5.93	16.03	4.23	0.36	~100
CZIF(Co_2Cu_2)	69.44	1.61	6.75	12.28	9.48	0.45	~100
CZIF(Co_1Cu_3)	71.62	1.42	5.94	6.28	12.91	0.34	~100
CZIF(Co_0Cu_4)	79.05	1.22	5.17	0	15.59	0.47	~100

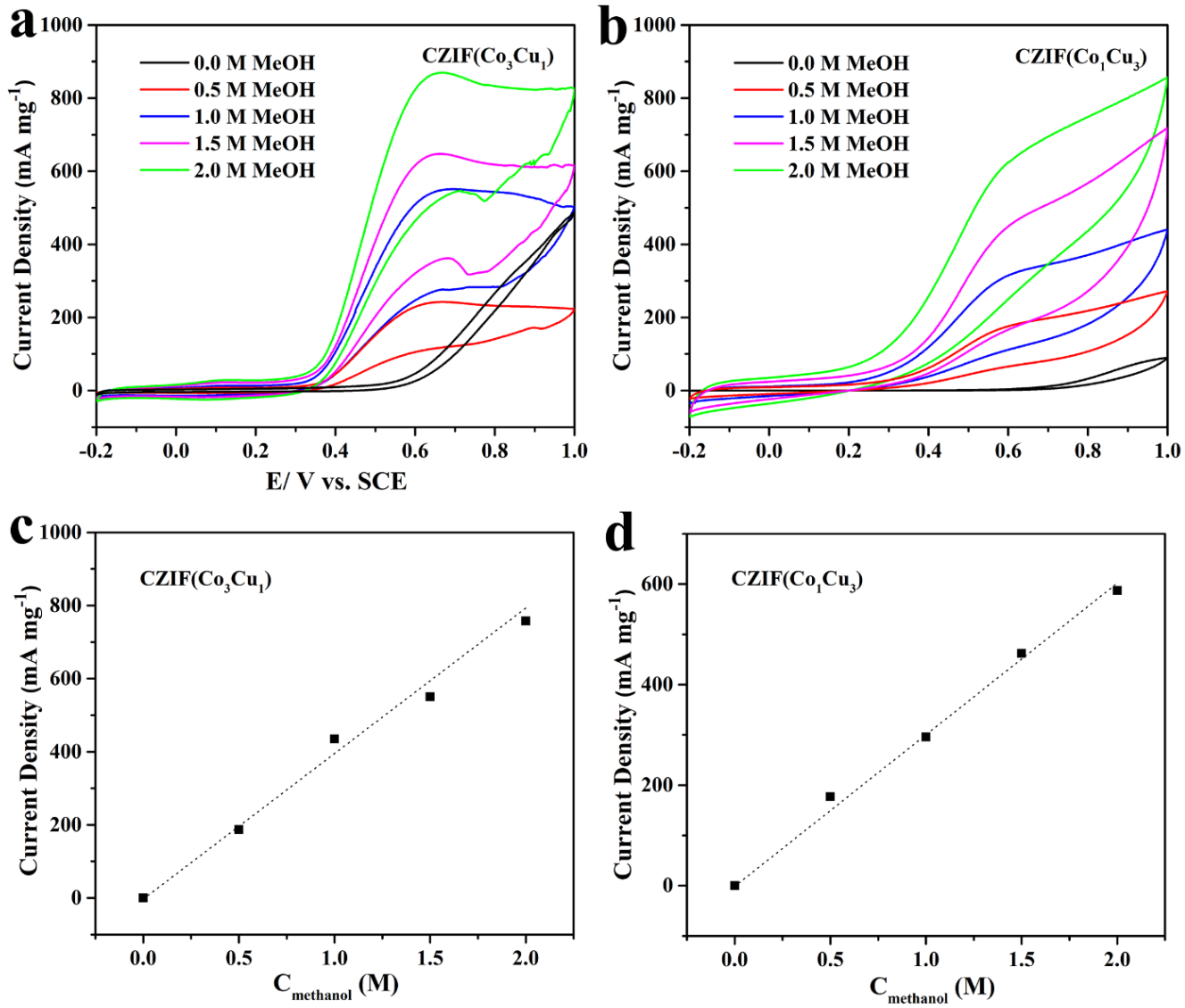

Figure S9. Cyclic voltammograms for MOR at scan rate of 50 mV s^{-1} over (a) CZIF(Co_3Cu_1) and (b) CZIF(Co_1Cu_3) in different concentrations of MeOH (0.0, 0.5, 1.0, 1.5 and 2.0 M) in 1.0 M NaOH solution. Plots of oxidation peak current density (after the baseline current obtained in 0 M MeOH is subtracted) versus concentrations of MeOH for (c) CZIF(Co_3Cu_1) and (d) CZIF(Co_1Cu_3).

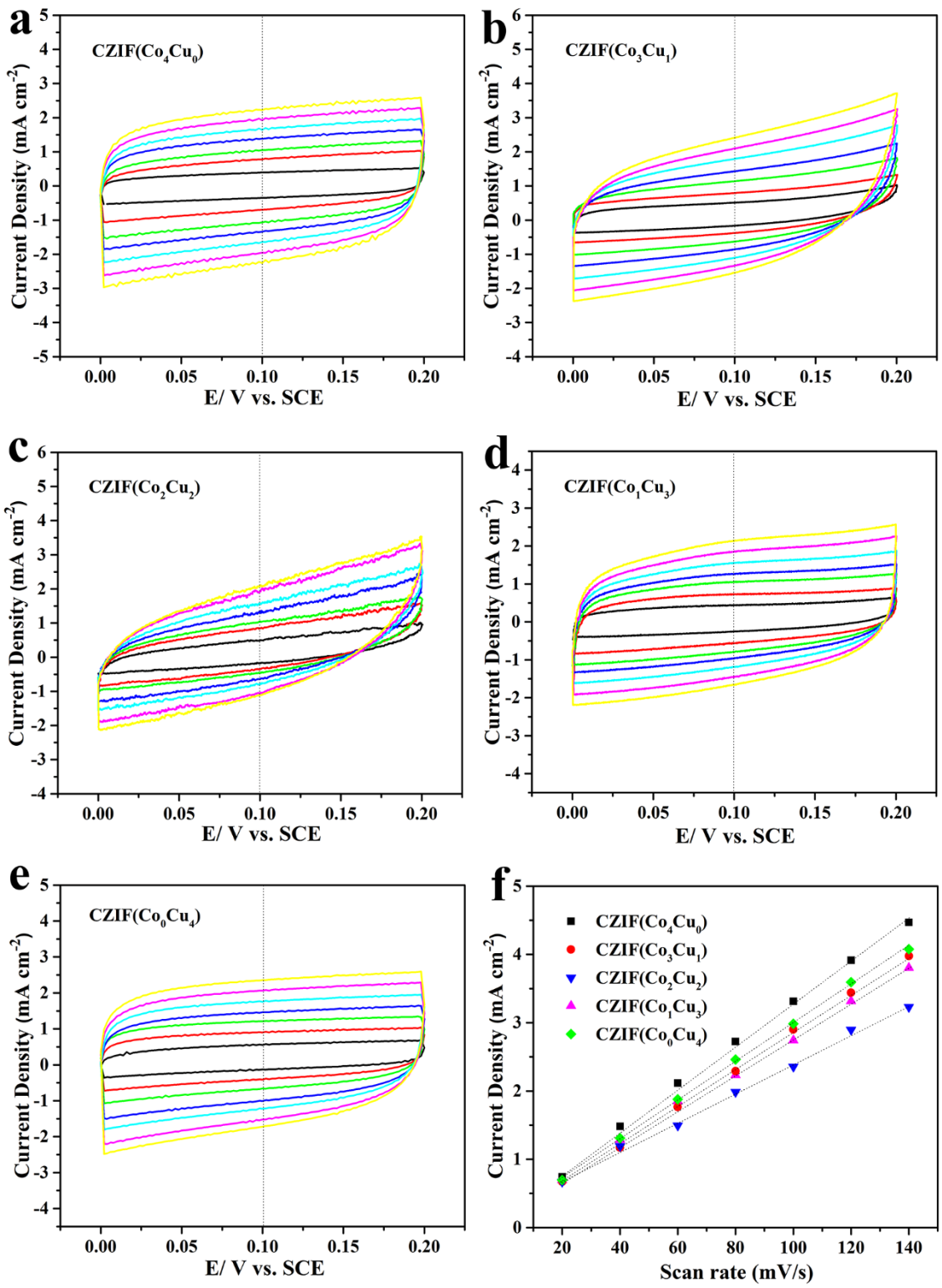

Figure S10. Capacitive current density obtained from double layer charging versus potential curves for: (a) CZIF(Co_4Cu_0), (b) CZIF(Co_3Cu_1), (c) CZIF(Co_2Cu_2), (d) CZIF(Co_1Cu_3), and (e) CZIF(Co_0Cu_4). Continuous cyclic voltammetry sweeps are conducted in the region without Faradic current to obtain the results. (f) Graphs of measured capacitive current versus scan rate for MOR over different CZIF materials. (The results shows that the current is linearly corelated with scan rate for both catalysts, indicating capacitive charging behavior in the regions of scan rates the measurements are carried out.)

Table S3. Comparison of the electrocatalytic activities of the different CZIF materials reported herein for MOR with respect to other non-precious and precious MOR electrocatalysts reported in the literature.

Catalysts	Experimental Conditions	Scan Rate (mV/s)	Peak Specific Current (mA/cm^2)	Peak Mass Activity (A/g)	References
CZIF(Co_3Cu_1)	**1 M KOH + 1 M MeOH**	**50**	**83.8**	**419**	**This work**
CZIF(Co_1Cu_3)	**1 M KOH + 1 M MeOH**	**50**	**62.1**	**310.6**	**This work**
$Ni_{0.75}Cu_{0.25}$	0.1 M KOH + 1.0 M MeOH	50	32	168	5
CUGU-15	1 M KOH + 1 M MeOH	50	29.8	527	6
NiP/rGO	1 M KOH + 0.5 M MeOH	10	16.4	117	7
NiCu	0.1 M KOH + 0.2 M MeOH	10	21	30	8
$NiCo_2O_4/Ni(OH)_2$	1 M KOH + 0.5 M MeOH	10	132	92.3	9
Co-MOF/GO	1 M KOH + 3.0 M MeOH	50	29.1	8.2	10
NiSn	0.5 M KOH + 0.5 M MeOH	50	50.9	819.3	11
Ni-Cu/C_3N_4	1 M KOH + 1.0 M MeOH	50	1.6	5.6	12
CoCuBi	1 M KOH + 1.0 M MeOH	100	118	-	13
Pt/C	1 M NaOH + 0.5 M MeOH	50	100	200	14
Pt-C_3N_4	1 M KOH + 0.5 M MeOH	50	1,83	150	15

Table S4. Measured electrochemical double-layer capacitances for a series CZIF materials.

	Samples				
	CZIF(Co_4Cu_0)	**CZIF(Co_3Cu_1)**	**CZIF(Co_2Cu_2)**	**CZIF(Co_1Cu_3)**	**CZIF(Co_0Cu_4)**
C_{dl} ($mF\ cm^{-2}$)	30.77	27.83	21.34	25.67	28.28

References

1. X. He, C. Yang, D. Wang, S. E. Gilliland, D.-R. Chen, W.-N. Wang, Facile synthesis of ZnO@ZIF core–shell nanofibers: crystal growth and gas adsorption, *CrystEngComm* **2017**, *19*, 2445-2450.

2. K. Kida, M. Okita, K. Fujita, S. Tanaka, Y. Miyake, Formation of high crystalline ZIF-8 in an aqueous solution, *CrystEngComm* **2013**, *15*, 1794-1801.

3. Y. Chen, S. Ji, Y. Wang, J. Dong, W. Chen, Z. Li, R. Shen, L. Zheng, Z. Zhuang, D. Wang, Y. Li, Isolated single iron atoms anchored on N-doped porous carbon as an efficient electrocatalyst for the oxygen reduction reaction, *Angew. Chem. Int. Ed.* **2017**, *56*, 6937-6941.

4. A. Han, B. Wang, A. Kumar, Y. Qin, J. Jin, X. Wang, C. Yang, B. Dong, Y. Jia, J. Liu, X. Sun, Recent advances for MOF-derived carbon-supported single-atom catalysts, *Small Methods* **2019**, *3*, 1800471 (1-21).

3. X. Cui, P. Xiao, J. Wang, M. Zhou, W. Guo, Y. Yang, Y. He, Z. Wang, Y. Yang, Y. Zhang, Z. Lin, Highly branched metal alloy networks with superior activities for the methanol oxidation reaction, *Angew Chem. Int. Ed.* **2017**, *56*, 4488-4493.

4. Y.-P. Wu, J.-W. Tian, S. Liu, B. Li, J. Zhao, L.-F. Ma, D. S. Li, Y.-Q. Lan, X. Bu, Bi-microporous metal-organic frameworks with cubane $[M_4(OH)_4]$ (M = Ni, Co) clusters and pore space partition for electrocatalytic methanol oxidation reaction, *Angew Chem. Int. Ed.* **2019**, *58*, 12185-12189.

5. H. Zhang, C.-D. Gu, M.-L. Huang, X.-L. Wang, J.-P. Tu, Anchoring three-dimensional network structured Ni-P nanowires on reduced graphene oxide and their enhanced electrocatalytic activity towards methanol oxidation, *Electrochem. Commun.* **2013**, *35*, 108-111.

6. R. Ding, J. Liu, J. Jiang, F. Wu, J. Zhu, X. Huang, Tailored Ni-Cu alloy hierarchical porous nanowire as a potential efficient catalyst for DMFCs, *Catal. Sci. Technol.* **2011**, *1*, 1406-1411.

7. B. Wang, Y. Cao, Y. Chen, R. Wang, X. Wang, X. Lai, C. Xiao, J. Tu, S. Ding, Microwave-assisted fast synthesis of hierarchical $NiCo_2O_4$ nanoflower-like supported $Ni(OH)_2$ nanoparticles with an enhanced electrocatalytic activity towards methanol oxidation, *Inorg. Chem. Front.* **2018**, *5*, 172-182.

8. R. Mehek, N. Iqbal, T. Noor, H. Nasir, Y. Mehmood, S. Ahmed, Novel Co-MOF/graphene oxide electrocatalyst for methanol oxidation, *Electrochim. Acta* **2017**, *255*, 195-204.

9. J. Li, Z. Luo, Y. Zuo, J. Liu, T. Zhang, P. Tang, J. Arbiol, J. Llorca, A. Cabot, NiSn bimetallic nanoparticles as stable electrocatalysts for methanol oxidation reaction, *Appl. Catal. B: Environ.* **2019**, *234*, 10-18.

10. I.S. Pieta, A. Rathi, P. Pieta, R. Nowakowski, M. Hołdynski, M. Pisarek, A. Kaminska, M.B. Gawande, R. Zboril, Electrocatalytic methanol oxidation over Cu, Ni and bimetallic Cu-Ni nanoparticles supported on graphitic carbon nitride, *Appl. Catal. B: Environ.* **2019**, *244*, 272-283.

11. D. C. Sesu, P. Marbaniang, S. Ingavale, A. C. Manohar, B. Kakade, Bi-Co-Cu metal oxide foam as significant electrocatalyst for methanol electrooxidation, *ChemistrySelect* **2020**, *5*, 306-311.

12. S. S. Mahapatra, J. Datta, Characterization of Pt-Pd/C electrocatalyst for methanol oxidation in alkaline medium, *Int. J. Electrochem.* **2011**, 2011, 563495.

13. M. Zhu, C. Zhai, M. Sun, Y. Hu, B. Yan, Ultrathin graphitic C_3N_4 nanosheet as a promising visible-light-activated support for boosting photoelectrocatalytic methanol oxidation, *Appl. Catal. B: Environ.* **2017**, 203, 108‑115.